Fast accurate multi-key weight measurement

Stefanie Gutschmidt[1] Mark McGuinness[2]
William Munn[3] James Hannam[4] Emma Greenbank[5]
Soomin Jeon[6] Chang-Ock Lee[7] Celia Kueh[8]
Tony Gibb[9] Ben Goodger[10] Andrew McIntyre[11]

(Received 16 June 2017; revised 5 April 2018)

Abstract

We consider an industrial problem brought to the Mathematics in Industry New Zealand study group in 2016, where items pass briefly over load cells resulting in a noisy oscillatory signal, from which the mass of the item is to be computed. We compare results obtained using a single load cell for one piece of fruit, with results from passing over two load cells in tandem or in succession with fruit on multiple keys. We develop mathematical models to assist with the computation of total load mass, considering both deterministic and statistical approaches. The fitting of simple harmonic motion plus a step function exhibits the possibility of rapid estimates of load mass. We find that using multiple

DOI:10.21914/anziamj.v58i0.12222, Published 2018-05-27, as part of the Proceedings of the 2016 Mathematics and Statistics in Industry NZ Study Group. ISSN 1445-8810. (Print two pages per sheet of paper.)

keys to measure the weight of a fruit provides more accurate results than using the single-key method.

Contents

1 Introduction

COMPAC designs and exports equipment that sorts fruits and products for orchard packhouses. They presented a challenge to the 2016 Mathematics in Industry New Zealand (MINZ) study group, entitled *Estimating the Weight*

of a Moving Article Across Multiple Weigh Points. COMPAC also presented challenges to MINZ and MISG (Mathematics in Industry Study Group) in previous years. For instance in the 2004 Study Group, the Compac challenges were "The Boxing Problem" and "The Bagging Problem" [1]. The former challenge was about filling boxes with a specific number of articles to specifications such as minimum weight and maximising the number of boxes packed. The "Bagging Problem" was about filling bags above a minimum weight and maximising the number of bags packed, amongst other criteria. In 2015 Compac brought another challenge to MINZ, entitled "Calibration Transform for Discrete Spectroscopic, Mechanical and Optical Systems". This project aimed at creating a calibration transform that would convert the output of different spectroscopic systems to a standardized form. In all these problems, including the Compac challenge described here, the MINZ or MISG teams built mathematical and computational models to understand and predict the physical situation and to improve and optimize algorithms for the processes. Solutions proposed by study group teams have directly impacted and significantly improved Compac's boxing, weighing, bagging, and sorting software processes, which led to increased quality and productivity of their equipment and systems.

The work presented here is based on the results of the MINZ 2016 study group. Part of the fruit sorting process relies on fruit being weighed as it briefly passes over load cells on a conveyer belt. The fruit is supported by holders or keys. The weighing table needs to be able to deal with a range of fruit sizes and geometries. For instance, some fruit in the proposed new design will be supported by a single holder or *key* that will be measured as the single key moves over a load cell, and previous conveyor belt designs used a single holder for a single piece of fruit. The new design of the weighing section has led to the possibility of having one piece of fruit or any other article on multiple keys, to allow each key to remain on a load cell for a longer period of time than in previous single-holder designs. COMPAC mainly sorts orchard fruit, but for the investigations in this paper articles not limited to fruits are used. Therefore we refer to articles when relating to the analysis of this

Figure 1: Articles on conveyor belt system: (a) single-key article (apple); (b) multi-key article (kumara).

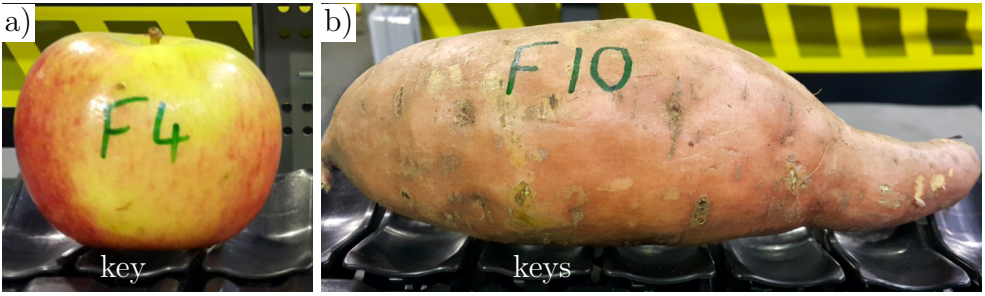

work and to fruits when referring to the purpose and application of COMPAC SORTING. Now, articles may rest on one or multiple keys (Figure 1), which are weighed sequentially, key-by-key. The main challenge arising from the proposed multi-key weighing process is the measurement of the distributed weight of the article by multiple keys, typically with unknown contact process machine is complicated by three effects: the multiple support points; that the article and/or the key may bounce during the weighing time; and the noise arising from the engineering environment. COMPAC are particularly interested in assessing whether the new design, with the help of some mathematical postprocessing of the data, is effective in improving the accuracy of the weighing process. COMPAC aims to measure masses accurate within 1 g for single-key and 5 g for multi-key articles.

We analyse and post-process data to find the most desirable weighing solution for COMPAC's existing measuring system. The analysis answers the following three key questions.

1. Currently, there are two measuring concepts (Section 1.1)—parallel and serial—by which articles are measured. Which of the two measuring set ups—single or dual load cell— provide a higher accuracy?

2. Can a mathematical model be developed that is able to estimate the true weight of the article from recorded data sets for all considered

articles—single and multi-key alike?

3. What is the estimated theoretical weighing accuracy for a given conveyor belt velocity?

1.1 Single key versus multiple keys

The simultaneous two-key or parallel weighing method measures the weight on a pair of keys that simultaneously pass over two load cells, and outputs signals from each of the load cell. The data used in our analysis is from a seven key set up illustrated in Figure 2. We refer to keys by consecutive number, with number 1 being the first key, and number 7 being the last. The support points of the keys are organised such that three keys (namely keys 2-4-6) are measured on load cell one and four keys (namely keys 1-3-5-7) are measured on load cell two. In this set up the keys are weighed simultaneously in pairs, excluding key 7 which has no pair; key 1 is weighed on load cell two simultaneously with key 2 on load cell one, and so forth.

In contrast, in the single-key or serial weighing method the keys pass over one load cell sequentially and due to the design of the weigh beam the single-key measurements are made in half the period of time that is available when using the parallel weighing method. Data obtained with the single-key method are generated by another load cell (load cell three, with a wider top plate) that is impacted by all seven keys (not shown).

The data we considered during the study group was obtained for a setup with just seven keys in total, which go over the weigh-bridge with three load cells, crossing them as detailed above, then loop around and go over it again. Fruit or test weights are added by hand to the keys, before they reach the weigh-bridge, and are removed after the weigh-bridge before the keys loop around to begin again. The placement of the article is repeated several times in one data run. Hence the data shows at various times either load cells with nothing on them, or with empty keys moving across them, or with a loaded

Figure 2: Key and load cell numbering system: (a) real system; (b) schematics.

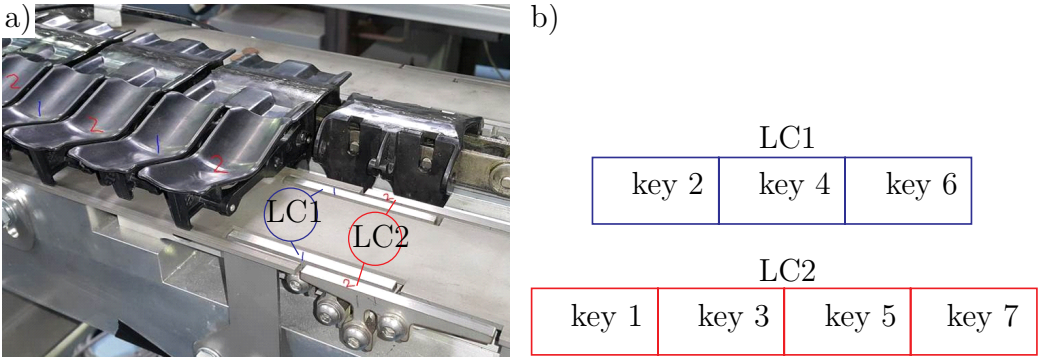

key moving across them. The mean signal value indicates the particular case at any given time. Both raw and filtered signals are available. The filter is a fifth-order Butterworth filter set at about 55 Hz.

COMPAC currently operates an automatic system that specialises in weighing fruits based on single-key technology. The method estimates the weight of the article by calculating the average of the low-pass filtered output signal from the load cell for a time range when the key and fruit passed over the load cell. An example is illustrated in Figure 3; key 2 has the mandarin on it; the other keys are empty but they weigh about 18 g. An estimation of the weight of a single-key article such as the mandarin using this average technique is within 0.3 g of its actual weight at this belt speed.

When the simultaneous weighing method is applied to a two-key sized fruit like a pear, there are two potential outcomes based on the position of the article or fruit on the key(s). In the first case the fruit is positioned such that the fruit lies on a key pair with each key simultaneously supported on a separate load cell as illustrated by the signal in Figure 4a. In the second case the fruit is positioned such that the key pair is measured in a staggered manner, each key being weighed in separate time windows and thus its weight is recorded sequentially instead of simultaneously as illustrated in Figure 4b.

Figure 3: Filtered load cell signals for a mandarin sitting on a single key, belt speed 900 rpm. The zero weight is arbitrary at about 220 g for both cells. An empty key weight gives a mass change of about 18 g; the mandarin a further 110 g approximately. Key 1 (load cell 2) is empty while passing over the load cell system together with the mandarin on key 2 (load cell 1) simultaneously. Key numbering is detailed in Figure 2.

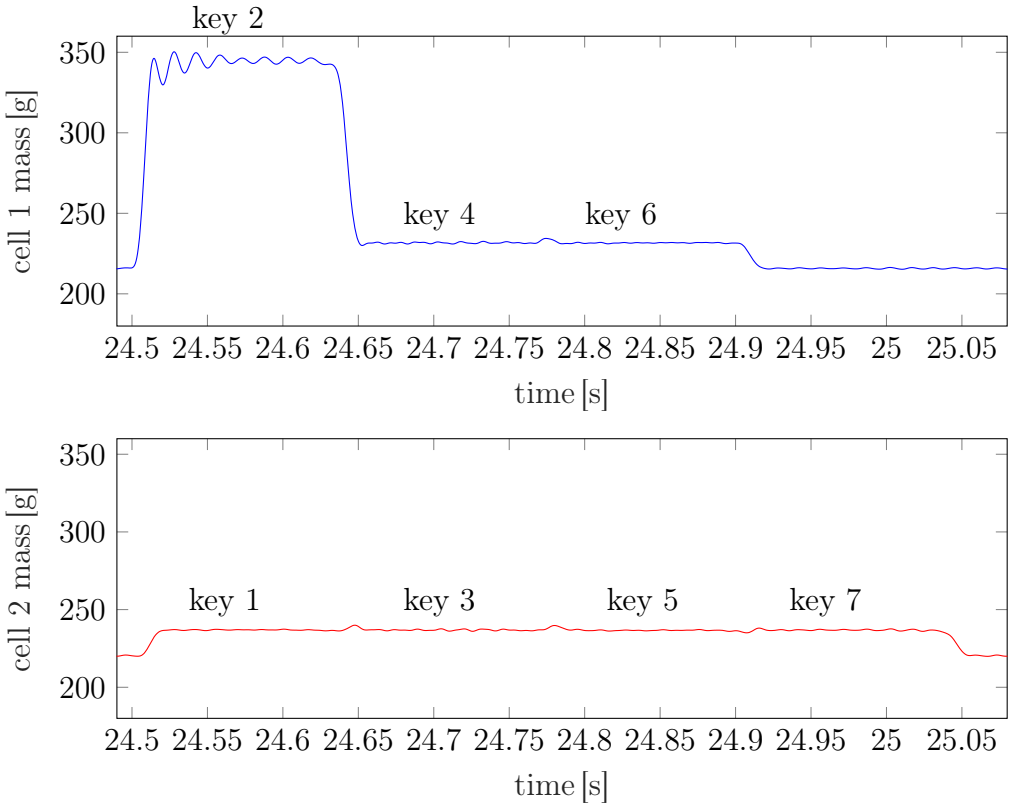

Figure 4: Load cell signals—mass versus time—for a pear positioned on two keys, belt speed 900 rpm.

(a) Simultaneous weight measure. The pear is mainly carried on key 4, but some of its weight is also on key 3, both measured during the same time range (23.9, 24.05) s. Lift-off of the fruit from the key is observed in the signal behaviour indicated by the black line.

(b) Staggered weight measure. The pear is mainly on key 2, weighed during the time period (66.3, 66.5) s, but apparently some part is bouncing onto key 3 during the next measuring period.

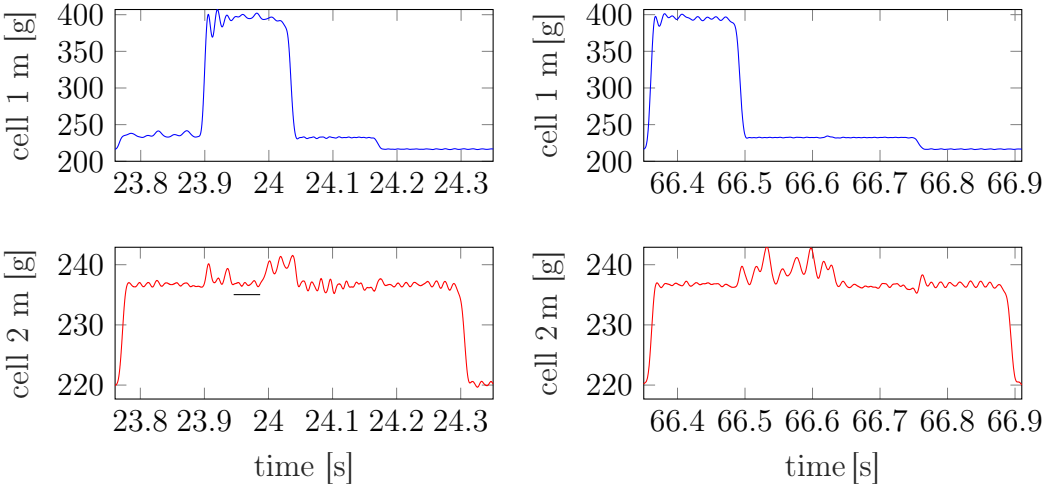

The motion of the keys over the load cells (and other obstacles) may cause the articles to bounce or rock on the keys and thus lift off one or more keys. If the lift-off happens entirely on one key, then the full weight of the fruit may be supported by the remaining key(s) for the duration of lift-off. If the article is in the process of shifting off or onto a key while it is passing over the load cell, then its weight might not register at all if it is 'in flight'. In this case the weight of a two-key article is estimated with the average method as a one-key article for the duration of the lift-off (Figure 4a). Applying this method the weight of the pear is estimated to be 165.11 g, whereas its actual

weight is 165.26 g (error 0.1%, or 0.15 g).

When a lift-off occurs such as in the second case, the prior method cannot be used as a shifting weight cannot be captured simultaneously on each load cell. We assume lift-off does not occur, and we treat the data as if the fruit is supported on one key. Then our prediction of the weight obtained by adding partial weights from two keys, falls outside the acceptable error tolerance of 1 g. However, measuring the weight of the pear in a staggered manner, assuming the article is resting on both keys 2 and 3, Figure 4b, the predicted weight is 164.2 g which also lies outside of the desired error tolerance. The importance of considering the aforementioned measuring methods, simultaneous and staggered, becomes more obvious when considering an article that spans more than two keys, as in Figure 5. In such a case it is impossible for the entire article's weight to be measured simultaneously.

The load cell voltage signals are statically calibrated by four different calibration masses ranging from 67.31 g to 200.03 g as well as with empty keys, which have slightly differing weights about 16.31 g. This is done for all three load cells. The calibration curves are linear and the calibration factors are directly implemented in our analyses. Unless otherwise specified we directly present measured masses in grams and not in voltage.

For an initial proof of concept of this method, time ranges were eye-balled manually at values after and before jumps. COMPAC SORTING monitors the speed of the belt in revolutions per minute (rpm) and the length of the keys is known by design. Furthermore, optical sensors are used to record when keys arrive at a load cell. Therefore, in an automated process the exact time ranges for when keys are on a load cell are readily available.

1.2 Data Analysis

The parallel setup (on two load cells) produces two simultaneous signals. In the data provided by COMPAC, as detailed above, a total of seven keys pass

Figure 5: Kumara weighing data, belt speed 900 rpm.

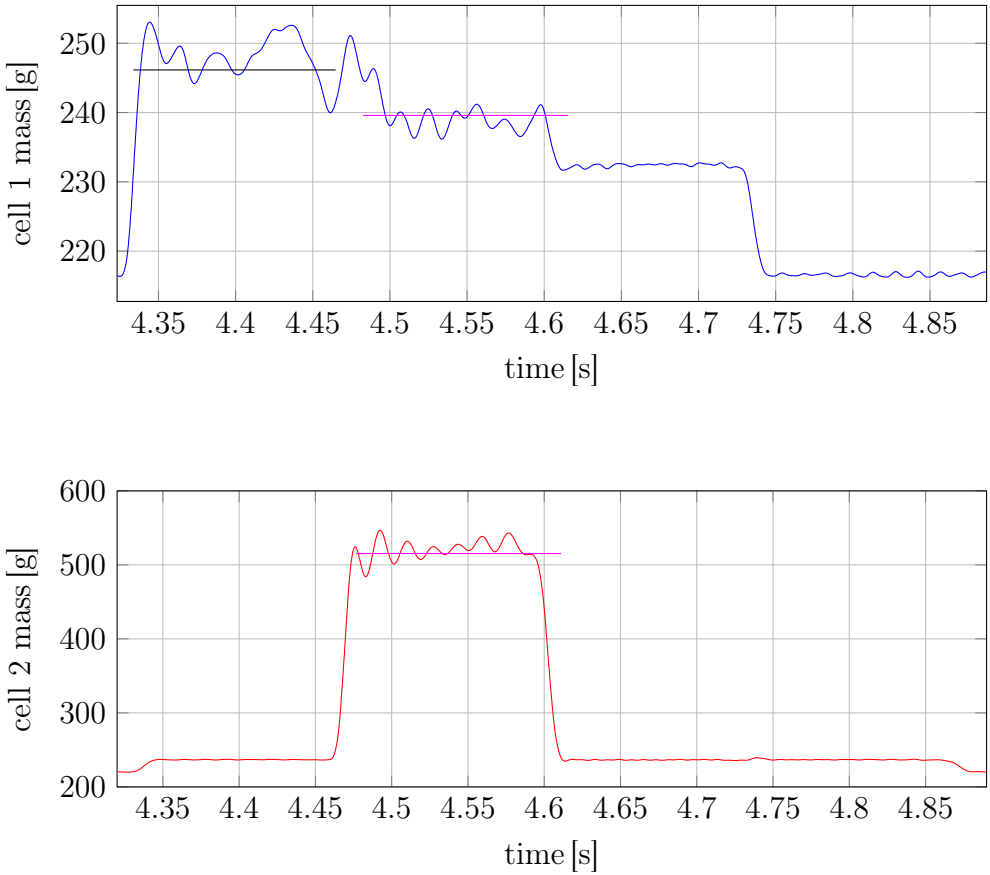

over the two load cells. The single load-cell setup produces one signal from seven keys in succession. We continue to use only the low-pass filtered signal that is provided directly from a load cell.

COMPAC currently operates equipment that weighs single-key fruit successfully. Their current method involves taking the average of the filtered signal from a load cell after initial transients have subsided. This method provides an estimated weight with under 1 g of error, for fruit that is not too heavy and for moderate belt speeds.

As discussed, when weighing a multi-key article, there are two possible scenarios for the article to pass over the load cells, namely simultaneously or successively. These cases result in qualitatively dissimilar signals, as the dynamic behaviour of keys dropping on to a load cell may cause fruit to move or even to bounce off a key for a short period of time. At the moment of lift-off for scenario one, the article's entire weight is assumed to be supported by the remaining key, from which an accurate measurement is obtained by using COMPAC's single-key method. However, should a lift-off occur for case two (successive measurement), the single-key method fails. Another degree of complexity is added by fruit bouncing between two or more keys due to the dynamic nature of the motion, which introduces transient signals due to impact and rebound and thus altering the apparent weight of the fruit.

Considering a multi-key article such as the kumara used in Figure 5, there are two ways of using an averaging technique to approximate the weight of a multi-key article. In each case, we take the average value of the signal $f(t)$ over some time window Δt starting from time t_0. By first adding the signals of the load cells together, and then taking an average of the combined signal we obtain an estimate for the weight of the article on each key pair and identify any simultaneously recorded dynamics. The total weight of the article is then estimated by adding up the estimates for each key pair. We refer to this method as the *combined signal* method. An alternative approach is to first split the load cell signals up into separate key signals and then take an average of the individual signals. Calculating the sum of the averages

Figure 6: Potato weights calculated using different weighing methods.

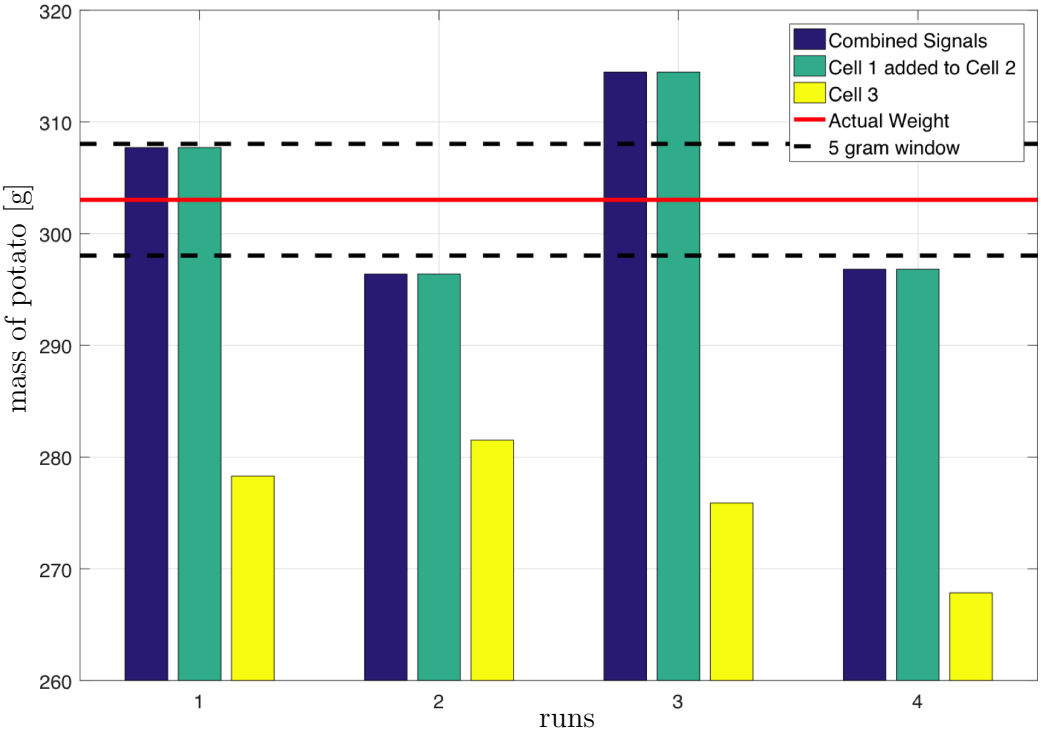

of all key signals provides an estimate of the total weight of the fruit. This method is referred to as the *separate signal* method. For the single-cell load cell measurement method (Section 1.1), the latter method for finding weight estimate must be used.

Testing these methods on a potato they were found to provide practically identical estimates. However, both estimates fall outside of the desired error tolerance of 1 g (Figure 6). The combined signal method and the separate signal method both produce better results from the parallel load-cell data than predictions estimated from the single load-cell data (Figure 6). This reveals a conclusion and answer to the first question of Section 1 about the

accuracy between parallel and serial load-cell measurement methods. The parallel load-cell set up provides higher accuracy measure than the single load-cell set up.

2 A Geometric Approach

In this section we consider a slightly different (geometric) approach to extract the weight from a raw load-cell signal that is oscillating due to damped harmonic motion. This approach largely follows that of Kesilmis and Baran [2]. We modestly extend their findings in the following three main ways:

1. by developing an explicit formula for the static equilibrium voltage;
2. by demonstrating the both linear and nonlinear interpolations give rise to the same solution for the static equilibrium voltage; and
3. by comparing these results with those obtained with a computer program that solves this problem using iterative methods.

The static equilibrium of a dynamic system is the mean value about which the object oscillates when in motion. For this highly dynamic weighing process of articles the mean value needs to be extracted from the signal. This off-set value is subject to change for every key and key-article combination.

The motivation for a geometric approach is as follows: the weight force that an article applies to the keys (and hence the load cell) typically causes the load cell to produce a voltage/time signal that resembles damped oscillations. Determining the equilibrium from the signal amounts to knowing the combined mass of the article of fruit, and the keys over which it spans (since the mass of an object on the load cell is linearly related to the voltage that the load cell outputs). Once this combined mass value is known, the masses of the keys (approximately 16 g each) are subtracted, giving the mass of the fruit.

To the extent that the voltage signals produced by the load cell can be

Figure 7: Linear interpolations to determine the off-set voltage.

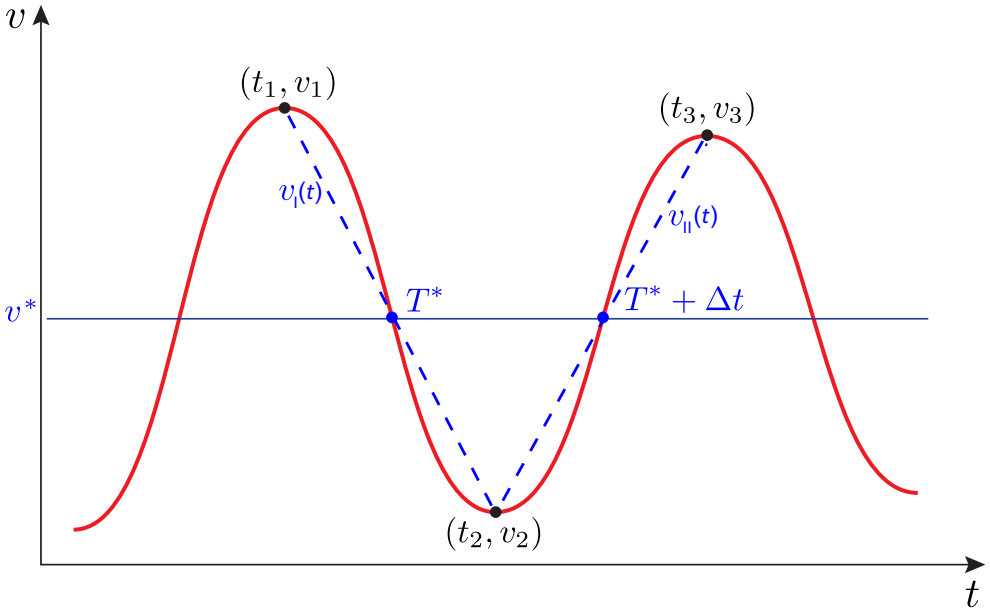

modelled by damped sinusoids, we exploit geometric properties of sinusoids to determine this off-set voltage. In the following we outline this method by referring to the details of Figure 7, which illustrates how this method is applied to a typical set of damped oscillations.

1. Locate three adjacent *local extrema* in the signal, with coordinates (t_1, v_1), (t_2, v_2), (t_3, v_3), where $v_i = v(t_i)$ for a voltage/time signal v.
2. Interpolate between t_1 and t_2 with a function $v_I(t)$, and again between t_2 and t_3 with a function $v_{II}(t)$ using either straight lines, or trigonometric functions.
3. Determine the special time, T^*, for which $v_I(T^*) = v_{II}(T^* + \Delta t)$ with $\Delta t = t_3 - t_2 = t_2 - t_1$ being the half-period of the oscillation.
4. Determine the off-set voltage, v^*, by evaluating $v_I(T^*)$.

The key for solving for both T^* and v^* is the assumption that the time intervals between the occurrence of each pair of local extrema is constant. In reality some variations would be present, but expected to be sufficiently small and therefore treated as negligible.

We now give a brief derivation of both linear and nonlinear 'interpolation' functions. Figure 7 illustrates how we interpolate using straight lines. For instance, the straight line joining (t_1, v_1) and (t_2, v_2) has a gradient of $v_2 - v_1/t_2 - t_1$. The line is described by

$$v_{\mathrm{I}}(t) = \left(\frac{v_2 - v_1}{t_2 - t_1}\right) t + \frac{v_1 t_2 - v_2 t_1}{t_2 - t_1} \quad \text{for} \quad t_1 \leqslant t \leqslant t_2 \,.$$

Similarly, the straight line that subsequently joins (t_2, v_2) and (t_3, v_3) is

$$v_{\mathrm{II}}(t) = \left(\frac{v_3 - v_2}{t_3 - t_2}\right) t + \frac{v_2 t_3 - v_3 t_2}{t_3 - t_2} \quad \text{for} \quad t_2 \leqslant t \leqslant t_3 \,.$$

These results agree with those of Kisilmis and Baran [2]. Imposing the geometric condition that $v_{\mathrm{I}}(T^*) = v_{\mathrm{II}}(T^* + \Delta t)$ and recalling that $\Delta t = t_3 - t_2 = t_2 - t_1$ gives

$$T^* = \frac{v_3 t_3 - 2v_3 t_2 + v_2 t_2 + v_2 t_1 - v_1 t_2}{2v_2 - v_1 - v_3} \,.$$

Then the offset voltage is

$$v^* = \frac{v_1 v_3 - v_2^2}{v_1 + v_3 - 2v_2} \,.$$

In order to see that this formula makes intuitive sense, consider the case of undamped motion. This has the consequence that $v_1 = v_3$. Replacing v_3 with v_1 in the expression for v^* yields

$$v^* = \frac{v_1^2 - v_2^2}{2v_1 - 2v_2} = \frac{(v_1 + v_2)(v_1 - v_2)}{2(v_1 - v_2)} = \frac{v_1 + v_2}{2} \,. \tag{1}$$

This demonstrates that v^* returns the correct value of the mean of the two local extrema v_1 and v_2, which represent a peak and a trough (in no particular order).

This formula for the off-set voltage is now derived in a slightly different manner. Instead of formulating *linear* interpolation functions v_I and v_{II}, we interpolate using portions of cosine functions. This is perhaps a slightly more intuitive approach, since we assume that the signals oscillate like sinusoids. The relevant interpolation functions in this case are

$$v_I(t) = \frac{v_1 - v_2}{2} \cos\left(\pi\left[\frac{t}{\Delta t} - \frac{1}{2\Delta t}(t_1 + t_2) + \frac{1}{2}\right]\right) + \frac{v_1 + v_2}{2} \quad \text{for } t_1 \leqslant t \leqslant t_2\,,$$

and

$$v_{II}(t) = \frac{v_2 - v_3}{2} \cos\left(\pi\left[\frac{t}{\Delta t} - \frac{1}{2\Delta t}(t_2 + t_3) + \frac{1}{2}\right]\right) + \frac{v_2 + v_3}{2} \quad \text{for } t_2 \leqslant t \leqslant t_3\,.$$

When we impose that $v_I(T^*) = v_{II}(T^* + \Delta t)$, we obtain

$$T^* = \frac{1}{2}(t_1 + t_2) + \frac{\Delta t}{\pi} \cos^{-1}\left(\frac{v_3 - v_1}{v_1 - 2v_2 + v_3}\right) - \frac{\Delta t}{2}.$$

If $\Delta t = t_3 - t_2 = t_2 - t_1$, then we obtain the same expression (1) for v^* as with the previous linear approach.

2.1 Results

The success of our formula for the off-set voltage, v^*, depends on the extent to which the actual voltage/time signals resemble damped simple harmonic motion. In many cases, but especially where articles are irregularly shaped, and appear to rock on their supporting keys, the signals display considerable volatility. In these situations, the value for v^* that the formula returns is also rather volatile.

An additional shortcoming of equation (1) for ν^* is that it assumes that the time between local extrema is constant, which is not always true in our data. As a result, we developed a computational method for solving the problem in a more rigorous manner. This method does not use interpolation functions, but operates on the data itself. It finds the particular time, T^*, for which the steady voltage is estimated by the formula

$$\nu_{\mathrm{I}}(\mathsf{T}^*) = \nu_{\mathrm{II}}(\mathsf{T}^* + \Delta\mathsf{t}) \tag{2}$$

where $\Delta\mathsf{t}$ corresponds to the "mean half-period" of the particular set of three local extrema. The raw data is discretised at intervals of 2.5×10^{-4} s, which slightly constrains the accuracy of both methods. This does not require that $\mathsf{t}_3 - \mathsf{t}_2 = \mathsf{t}_2 - \mathsf{t}_1$. Figures 8a to 8d contrast the results of applying both the expression, and the computational method, to the signals from two man-made articles (A1 and A4), and also from two real articles (F3, an orange weighing 290.0 g, and F8, a potato weighing 74.7 g).

Several key observations arise from Figure 8. The first is that both methods return similar values. The mass for A1 is estimated to be 75.85 g (using formula (1) for ν^*) and 75.38 g (using computational method (2) for ν_{I}). The mass for A4 is estimated to be 188.99 g (using ν^*) and 188.59 g (using ν_{I}). The mass for F3 is estimated to be 272.6 g (using ν^*) and 271.6 g (using ν_{I}). The mass for F8 is estimated to be 72.4 g (using ν^*) and 73.1 g (using ν_{I}). However, these results fall outside the acceptable tolerance of 5 g (for multi-key articles), as for example the true masses of articles A1 and A4 are 80.8 g and 200.1 g respectively.

The second observation is that the formula (1) derived for ν^*, even though it assumes incorrectly that the 'half-periods' between successive local extrema are equally spaced, returns a less variable value for the off-set voltage, which is useful as the values of ν^* are averaged in order to produce a single voltage for a given article (and, therefore, a single mass). Indeed, the expression (1) for ν^* often seems to smooth the volatility of the numerical solution; this is especially apparent in the case of article A1.

Figure 8: Examples of applying the geometric method to filtered raw signals from load-cell data. Data is represented by the blue dot symbols, the numerical steady-state by solid black lines, and the formula steady-state by dashed red lines.

(a) Geometric approach applied to article A1.

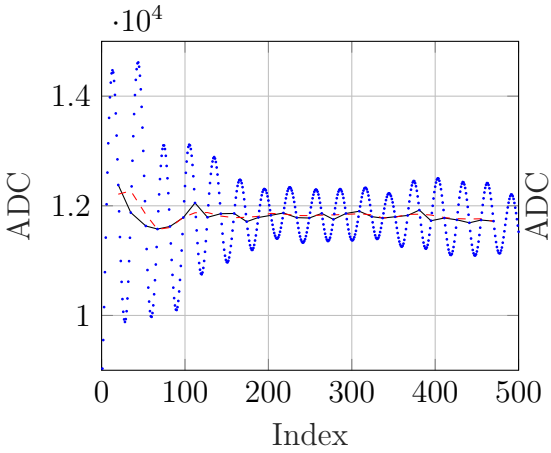

(b) Geometric approach applied to article A4.

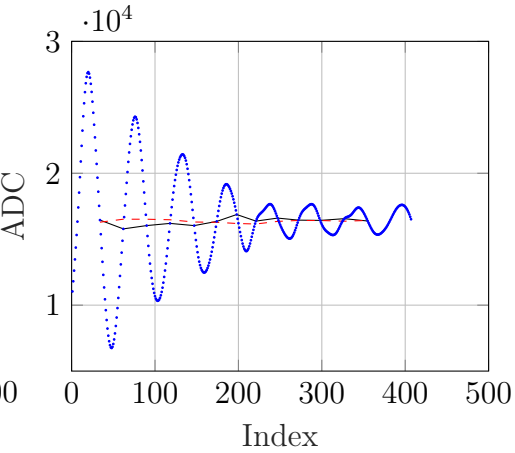

(c) Geometric approach applied to article F3.

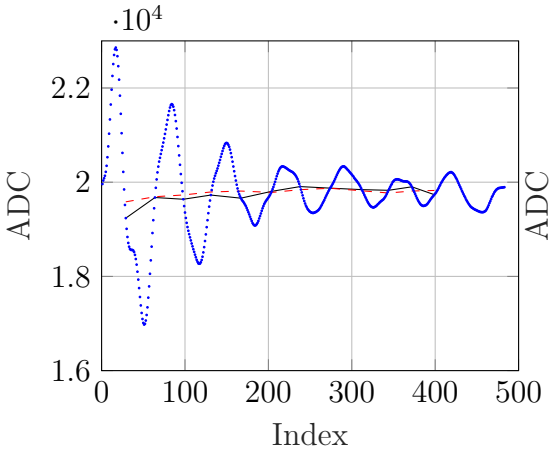

(d) Geometric approach applied to article F8.

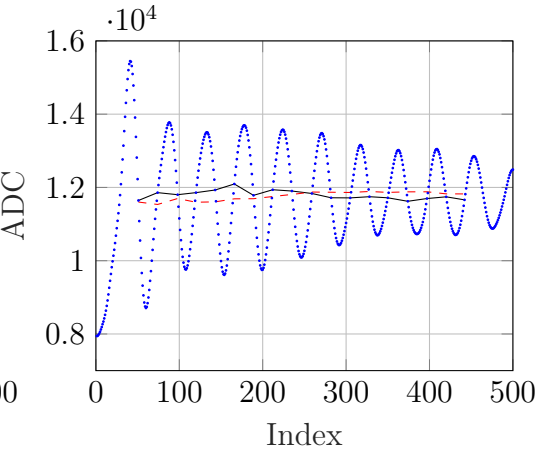

Overall, a geometric approach seems to hold some promise in solving the problem of high-speed weighing. In the case of an article that spans multiple keys, where there is sudden and unpredictable rocking or bouncing on keys, the signal may be sufficiently volatile that a geometric approach needs to be combined with another method. The application of these methods to signals where the article is known to rock or bounce should be the subject of further research in this area.

3 Nonlinear Fitted Solution Approach

In this section we consider an alternative and more sophisticated approach to those presented in previous sections, this time working directly with the raw (unfiltered) signal from any single load-cell as shown in Figure 9. The measured signal is the voltage from the load cell, converted from analogue to digital, and labelled ADC.

The signal plotted in Figure 9 consists of two major components: one is a step function; and the other is highly oscillatory. The former originates from the change of weight sensed by the load cell. Empty keys also cause a small impulsive change of voltage due to the change of sensed weight when the key first meets the load cell. For keys supporting an article this jump is significant and easy to identify. The oscillations are initiated by keys mechanically loading or unloading the load cell, and the resulting oscillation reveals the natural frequency of the load cell.

We seek to use nonlinear optimisation to fit the signal simultaneously with a step function and a damped harmonic motion solution. For simplicity of presentation, we consider only one load-cell signal in this section, and the focus is on an effective method for rapidly filtering out the oscillations in the signal.

Figure 9: Unfiltered input signal. The lower plot is a zoom-in on the time range $[24, 24.5]$ of the upper plot to show more detail.

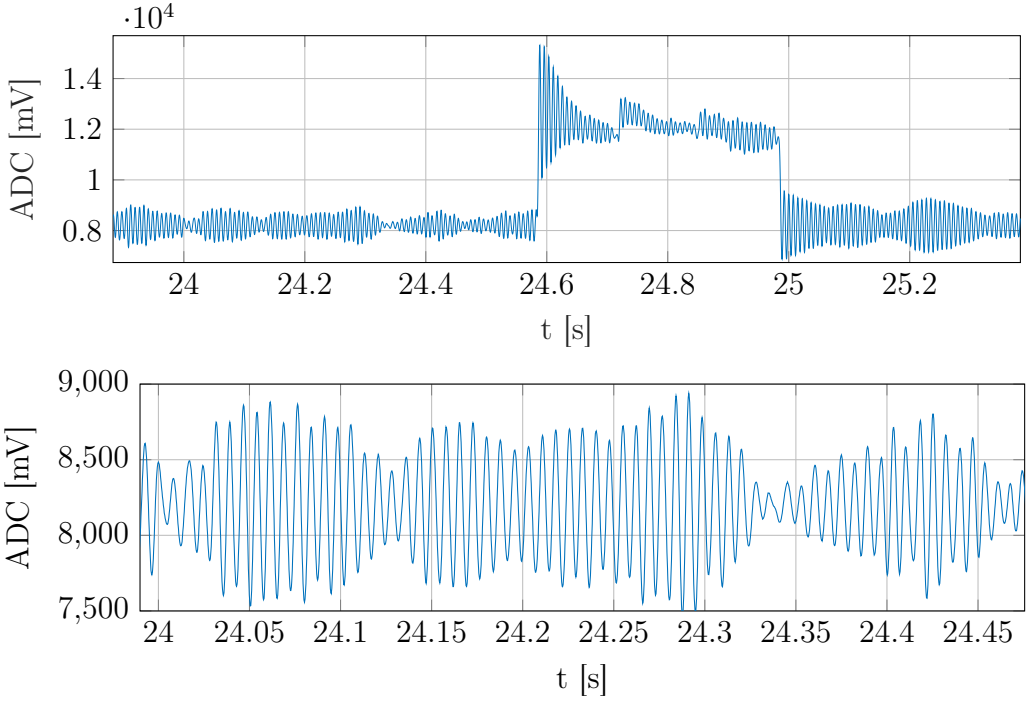

3.1 Mathematical modelling

Looking at Figure 9, we think of the signal y from a load cell as being composed of a static component y_s and a dynamic component y_d from the raw signal y_0,

$$y(t) = y_s(t) + y_d(t). \tag{3}$$

We envisaged that the dynamic component y_d might be separated from the static component y_s, which would be used for the determination of weight. To obtain the dynamic component of the signal y_d, we assume that it is

described as damped free vibration. Then, the dynamic component of the signal y_d satisfies the equilibrium equation of forces for damped free vibration or simple harmonic motion. The damped free vibration of the system is governed by the ordinary differential equation (ODE)

$$m\ddot{y}_d + b\dot{y}_d + ky_d = 0\,, \tag{4}$$

where m is the total effective oscillating mass, b is the damping coefficient, k is the effective spring constant of the load cell system, and overdots denote time derivatives.

Dividing the ODE (4) by m,

$$\ddot{y}_d + B\dot{y}_d + Ky_d = 0\,, \tag{5}$$

where $B = \frac{b}{m}$ and $K = \frac{k}{m}$. The general solution to (5) is

$$y_d(t) = A\, e^{-Bt/2} \cos(\Omega t + \varphi), \tag{6}$$

where the natural frequency of oscillation is $\Omega = \sqrt{K - B^2/4}$, and A and φ are arbitrary constants, determined by initial conditions. A is the initial amplitude of the oscillation, and φ is the phase shift (rad).

Now, we seek values for the parameters A, B, Ω, and φ of the dynamic component y_d and the static component y_s which provide the best fit to the given raw signal data y_0. Since a new damped oscillation is generated each time a carrier key passes over a load cell as shown in Figure 9, there are big jumps in the values of signals at these points. Therefore, we consider piecewise processing of the load signal over a time interval for fitting the data.

3.2 Moving window processing

Consider the kth time window T_k centered on the time value $t_{k,c}$ as shown in Figure 10. Each window covers $2n + 1$ samples of data and consecutive

Figure 10: Description of the moving windows.

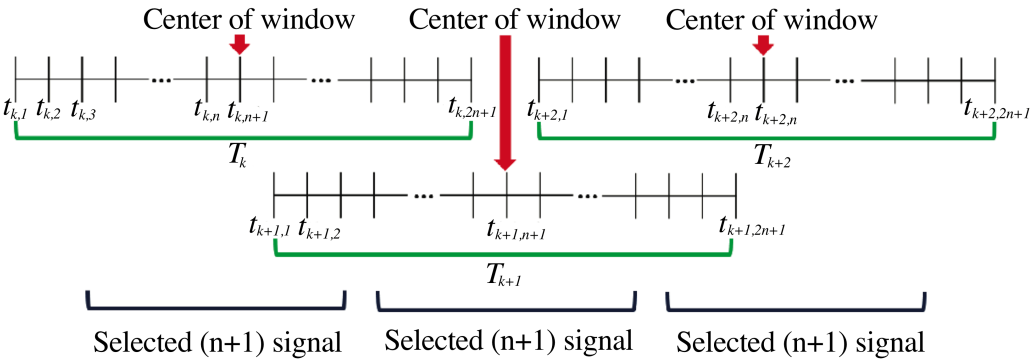

windows overlap by n data points. To reconstruct the signal on each window, we use $2n+1$ samples on each window for fitting, and we choose the middle $n+1$ values from the resulting fitted signal for reconstruction. Let $t_{k,a}$ and $t_{k,b}$ be lower and upper bounds of the time window T_k, respectively, then

$$t_{k,a} = t_{k,1} \leqslant t_{k,2} \leqslant \cdots \leqslant t_{k,c} = t_{k,n+1} \leqslant \cdots \leqslant t_{k,2n+1} = t_{k,b}.$$

This is a nonlinear least squares problem over each time window T_k. The least squares error S_k over the time window T_k is

$$S_k(A, B, \Omega, \varphi, y_s) = \sum_{i=1}^{2n+1} |y(t_{k,i}) - y_0(t_{k,i})|^2 . \tag{7}$$

We call the piecewise processing of the load signal the moving window process (Figure 11).

3.3 Nonlinear data fitting

We apply the Levenberg–Marquardt algorithm [3, 4] for solving the nonlinear least squares minimization problem on each window. This algorithm is a

Figure 11: Description of moving window process.

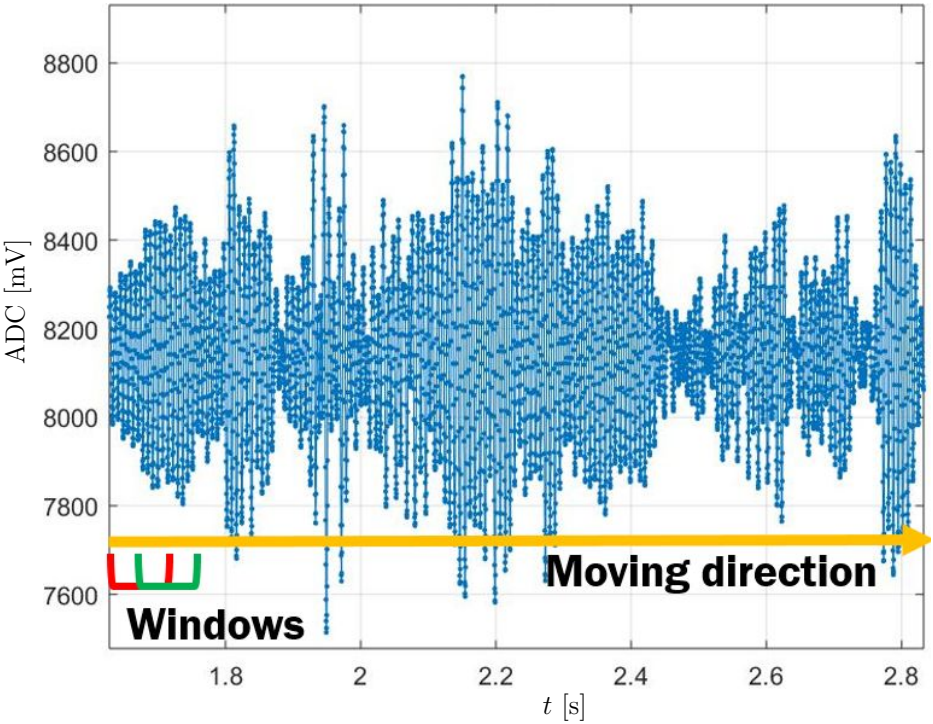

combination of the Gauss–Newton algorithm and the method of gradient descent. While it is more robust than the Gauss–Newton algorithm, it is usually slower to converge. It is important to begin with an initial guess that is close enough to the correct minimising value, for convergence to the global minimum.

3.3.1 Estimation of the static component

For the static component y_s, we adopt the average value of the raw signal over kth time window T_k as an initial value. On each window T_k, an initial

value is estimated as

$$y_s(T_k) = \text{average}\{y_0(t_{k,1}), y_0(t_{k,2}), \ldots, y_0(t_{k,2n+1})\}.$$

3.3.2 Estimation of the dynamic component parameters

The dynamic component of the signal $y_d(T_k)$ is obtained by subtracting $y_s(T_k)$ from $y_0(T_k)$. To find the dynamic component parameters using the Levenberg–Marquardt algorithm, we need to start with a good estimate of the initial value of each parameter.

The derivatives $\dot{y}_d$ and $\ddot{y}_d$ are replaced by estimates based on numerical differences, so that equation (5) is approximated by the system of equations

$$\begin{bmatrix} y_d(t_{k,a}) & \dot{y}_d(t_{k,a}) & \ddot{y}_d(t_{k,a}) \\ \vdots & \vdots & \vdots \\ y_d(t_{k,b}) & \dot{y}_d(t_{k,b}) & \ddot{y}_d(t_{k,b}) \end{bmatrix} \begin{bmatrix} K \\ B \\ 1 \end{bmatrix} = \begin{bmatrix} 0 \\ \vdots \\ 0 \end{bmatrix}. \tag{8}$$

The linear system (8) is rewritten as

$$M \begin{bmatrix} K \\ B \end{bmatrix} = \mathbf{f}, \tag{9}$$

where M is an $(2n+1) \times 2$ matrix and $\mathbf{f} \in \mathbb{R}^{2n+1}$. We then find initial estimates of K and B by solving the 2×2 normal equation

$$M^T M \begin{bmatrix} K \\ B \end{bmatrix} = M^T \mathbf{f}.$$

An estimate of parameter A is found from the maximum of $y_0 - y_s$ within the time window T_k as

$$A = \max_{t_{k,i} \in T_k} |y_0(t_{k,i}) - y_s(t_{k,i})|.$$

The initial frequency is estimated using

$$\Omega = \sqrt{K - B^2/4}\,.$$

The initial phase shift is estimated using

$$\varphi = \cos^{-1}\left(\frac{y_d(t_{k,a})}{A}\right).$$

Using the above estimates as an initial guess, we solve the minimisation problem (7) to reproduce the signal $y(T_k)$ by the Levenberg–Marquardt algorithm. The reproduced signal $y(T_k)$ is shown in Figure 12, during a time when there is no key on the cell. The fitted step values are relatively close to each other, indicating a reasonably stable filtered signal value for the zero additional load case.

3.4 Results

We apply our algorithm to data for a potato to illustrate the performance of the proposed approach. The potato has a true weight of 303.03 g. As shown in Figure 13, the signal is highly oscillatory even when empty carrier keys are passing over the load cells.

Relatively high-valued peaks occur when a carrier key supporting an object is on a load cell. There are three peaks visible in the given data and we indicate them using the numbered red arrows in Figure 13. The signals of the corresponding time intervals are shown in more detail in Figure 14.

To fit the potato data, we use a window size of 101 data values, and the size of the intersection between consecutive windows is 50 sampled points. Since the potato data is sampled every 0.25 ms, each window covers a time interval of about 25 ms.

Figure 15 shows the graph of the reproduced signal obtained by using our approach. The zoom-in graphs of the reconstructed signal on the time

Figure 12: Result of the deterministic approach, after fitting simple harmonic motion (red symbols) to raw data (black curve). The fitted step values approximating the mass, which can be regarded as a filtered signal, can also be seen (horizontal blue lines), for three windows.

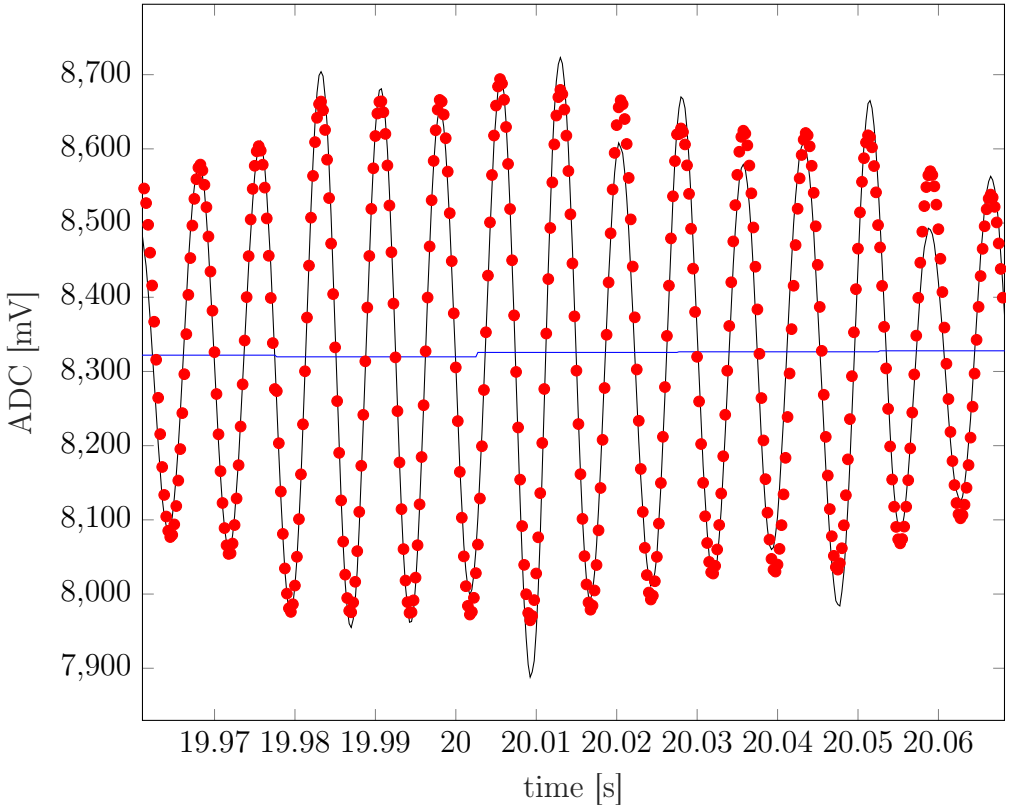

Figure 13: The load cell data obtained using a potato travelling at 900 rpm, with arrows showing the approximate location of the four intervals chosen for analysis. The earliest interval chosen has nothing on the keys, and the other three are when the potato is on the keys crossing the load cells.

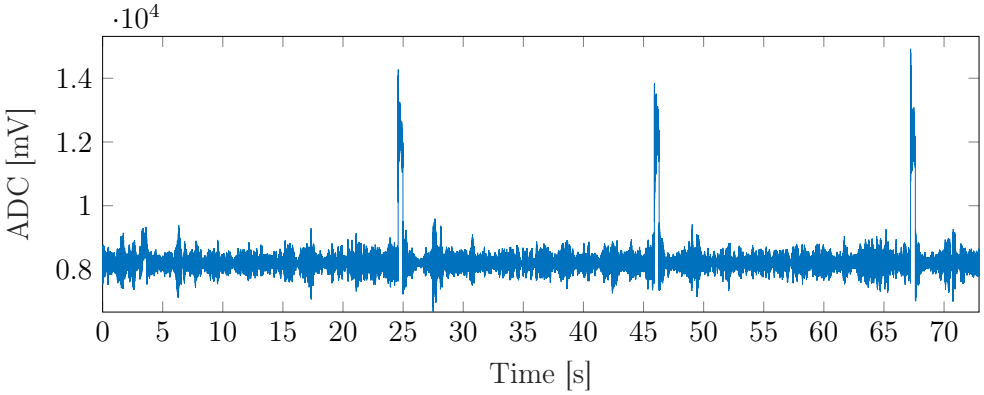

intervals 12.60–13.00 s, 24.58–24.98 s, 45.90–46.30 s, and 67.21–67.61 s are given in Figures 16 to 19, respectively. The black line indicates the original input signal, the red dots are the points on the reproduced signal, and the blue line shows the static component y_s obtained on each window.

Table 1 shows the static component values of the fitted signal for each of the time intervals (1) 12.60–13.00 ms, (2) 24.58–24.98 ms, (3) 45.90–46.30 ms, and (4) 67.21–67.61 ms. We use the average of these values for each key, and the static calibration formula

$$y = 37.8\,x + y_0$$

where y_s is the signal in mV when a loaded key is on the load cell, y_0 is the signal when an empty key is on the load cell, and x is the added mass in grams, to convert to a predicted weight for the potato by adding the masses on each of the three keys, since each key bears some part of the total weight of the potato. The three loaded events gave total masses of 309, 299, and 298 g respectively, for the mass of the potato, averaging to 302 ± 6 g. Comparing this to the static measured mass of 303 g, the individual amounts have an

Table 1: The static component of the reproduced signal on each window. The time intervals are: (1) 12.60–13.00 s; (2) 24.58–24.98 s; (3) 45.90–46.30 s; and (4) 67.21–67.61 s.

Time interval	(1)	(2)	(3)	(4)
Scale for $\mathtt{y}_\mathrm{s}$	10^3	10^4	10^4	10^4
$\mathtt{y}_\mathrm{s}$ [mV]	8.20	0.88	1.01	0.82
	8.19	1.24	1.22	1.16
	8.20	1.27	1.22	1.23
	8.20	1.26	1.21	1.23
	8.20	1.24	1.19	1.21
	8.20	1.22	1.18	1.20
	8.20	1.21	1.17	1.18
	8.20	1.20	1.16	1.17
	8.20	1.19	1.15	1.16
	8.20	1.19	1.15	1.15
	8.20	1.18	1.15	1.15
	8.19	1.23	1.22	1.16
	8.19	1.27	1.26	1.24
	8.19	1.26	1.25	1.25
	8.20	1.24	1.23	1.23
	8.20	1.22	1.21	1.21
	8.20	1.21	1.20	1.20
	8.20	1.21	1.20	1.19
	8.20	1.21	1.20	1.19
	8.20	1.21	1.20	1.19
	8.20	1.20	1.19	1.18
	8.19	1.21	1.22	1.18
	8.20	1.22	1.25	1.22
	8.20	1.21	1.24	1.24
	8.20	1.21	1.23	1.23
	8.20	1.19	1.21	1.21
	8.20	1.18	1.20	1.20
	8.20	1.17	1.19	1.19
	8.20	1.17	1.19	1.18
	8.20	1.17	1.19	1.18
	8.20	1.17	1.19	1.18
	8.20	1.16	1.18	1.17
Average	8.20	1.20	1.20	1.18

Figure 14: Expanded views of the four time intervals chosen to analyse a potato at 900 rpm, as shown in Figure 13. The first interval shows the baseline signal when keys are empty.

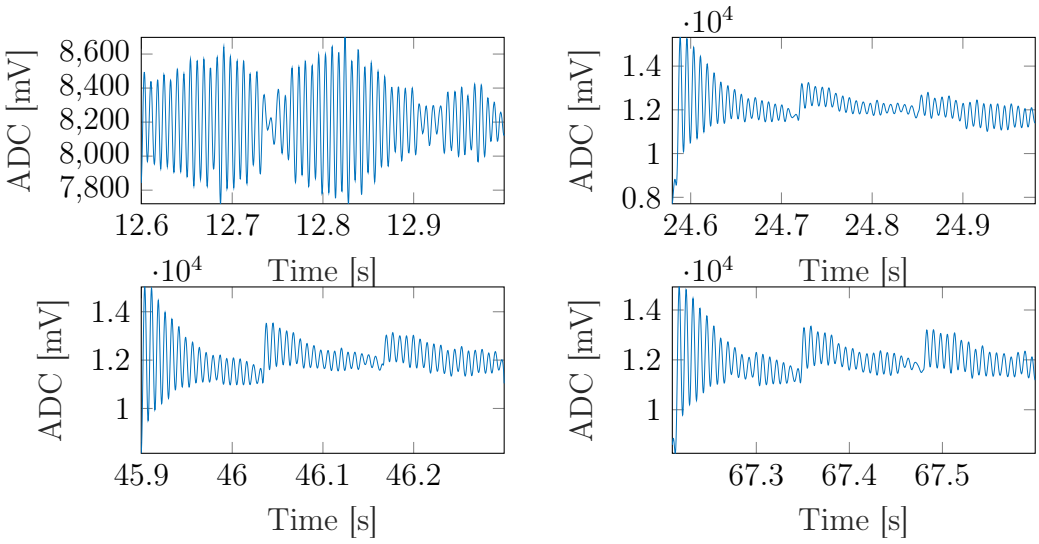

error of up to 6 g, whereas the average of the three runs is within 1 g of the true mass.

4 Statistical Approach

Thematically, we thought about gaining as much prior information about the individual articles as possible before they hit the load cells. This is made possible through the vision technology that COMPAC implement. COMPAC currently use a camera to photograph an article moving at high speed. The image is rapidly processed to determine characteristics such as the diameter, and any external deficiencies such as discolouration that might be present. This complements the weighing process in informing packers as comprehensively

Figure 15: Fitted signal y_d (red symbols), and fitted step functions y_s (blue lines, which look like spikes on this scale) for the potato data set. Three loaded key events are visible as spikes that were previously marked with arrows in Figure 13. The filtering performed in getting the blue lines y_s also identifies the single time interval when empty keys pass over the weigh table, near $t = 3\,s$ early in the time series.

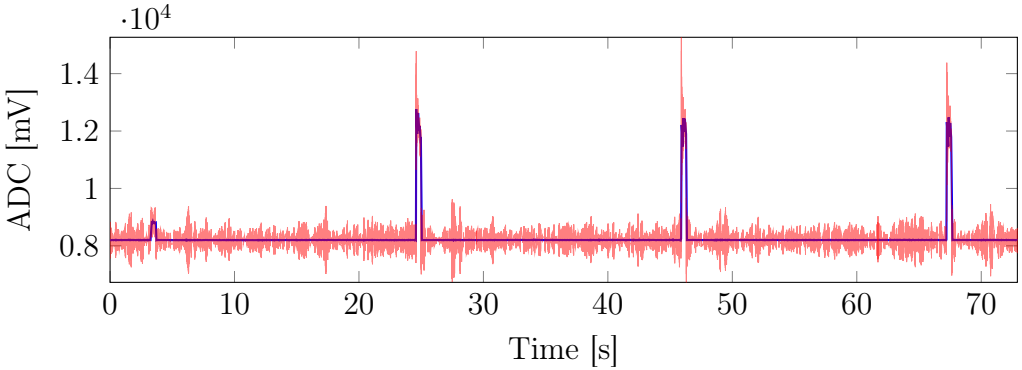

Figure 16: Results of fitting simple harmonic motion plus a step function on moving windows to the potato data from a load-cell. The data is generated by the same potato, crossing the load-cell three separate times. Data is a black solid line, the fitted signal y_d is red symbols, and fitted step functions y_s are solid blue lines. *Fits for 12.6–13.0 s with no load on the cell.*

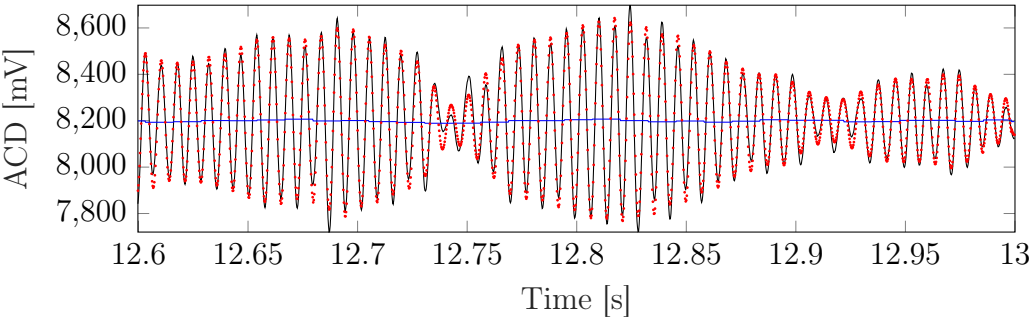

Figure 17: As for Figure 16: Fits for 24.58–24.98 s with keys loaded.

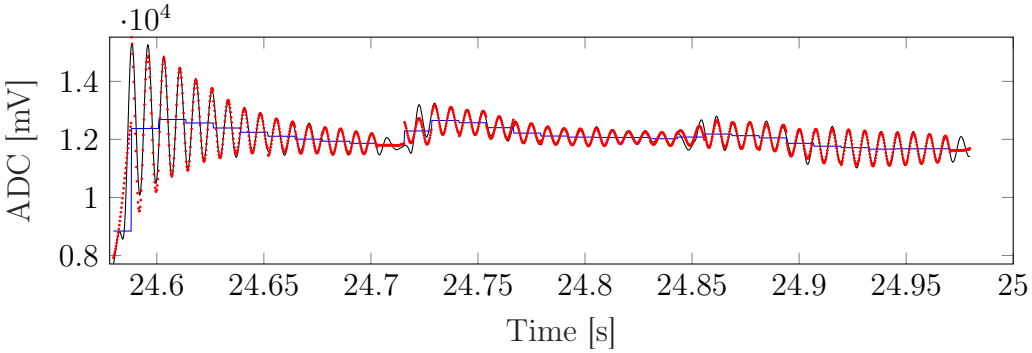

Figure 18: As for Figure 16: Fits for 45.9–46.3 s with keys loaded.

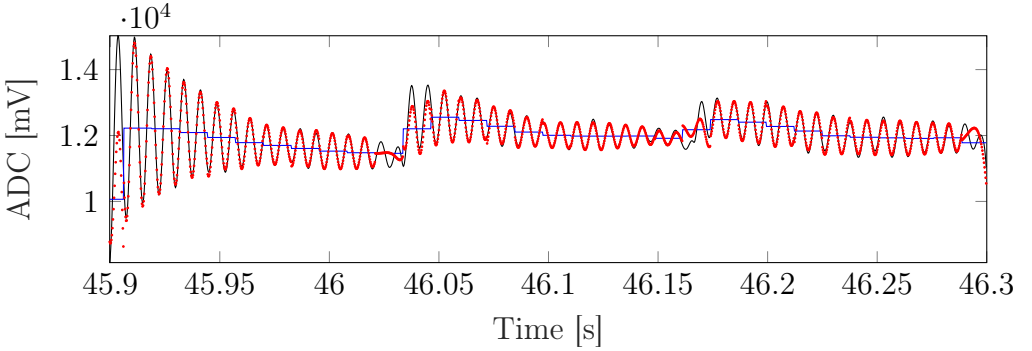

as possible. We posit two specific approaches to using this prior information. A simple top down photograph of an article of fruit is sufficient to generate a crude approximation to the mass of that article. For example, it is a simple task computationally to fit an ellipse to the outline of a piece of fruit, infer a three dimensional envelope of an ellipsoid, and then use an approximate value for the density of the article to estimate its mass. A typical density range across different types of fruit is 10^2–$10^3\,\mathrm{kg/m^3}$.

Even the fairly crude approximation of the mass that this process would

Figure 19: As for Figure 16: Fits for 67.21–67.61 s with keys loaded.

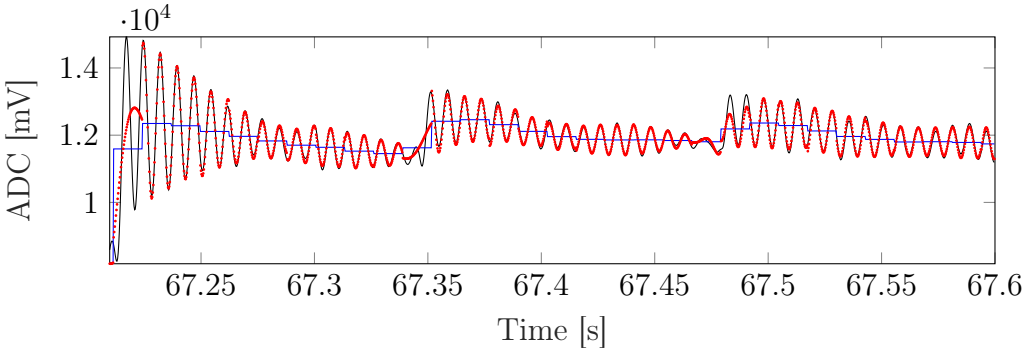

Figure 20: Decision matrix.

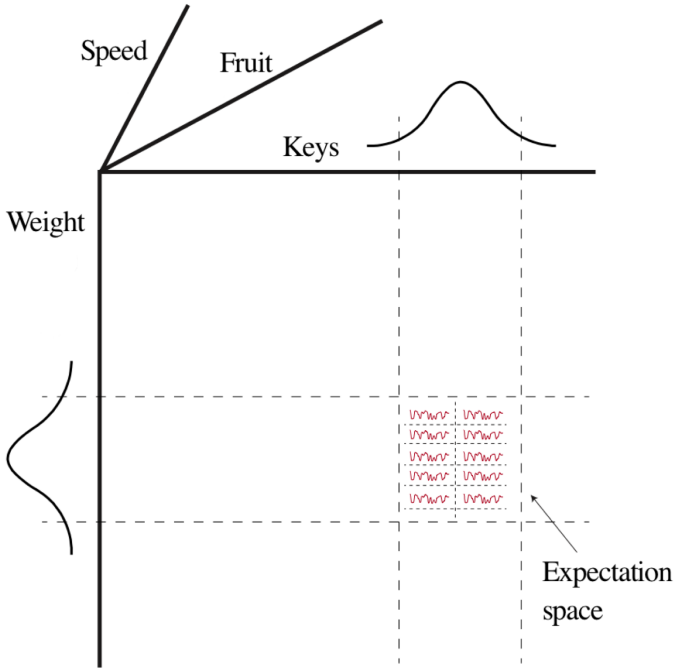

produce would be useful, for example as an initial estimate of mass in a parameter-fitting approach like the Levenberg–Marquardt method discussed in Section 3.3. At the moment, the signals that the load cells are producing are essentially the sum of an idealised step function, representing the true mass of the article being weighed, as well as noisy oscillations, caused by the natural oscillatory motion of the article as it bounces and rocks on the keys and load cells. Using the approximate mass value, a physical model is used to give a simple harmonic signal, which when backed out of a noisy signal will give us a better estimate of the true mass of the article.

Our second approach does not assume an accurate physical model for the motion of the article. Instead, a search is made on a data base of averaged signals, accumulated over time, each average corresponding to the specific type of article being weighed and a specific combination of keys on which it rests. Prior knowledge, before the load cell measurement, includes the type of the article, the estimated weight, the number of keys that are being spanned (but not necessarily touched) by the article, and the chain speed. This information defines a multi-dimensional expectation space in the multi-dimensional data space of averaged signals in our library. The current load cell output is cross-correlated to all entries in the expectation space, with one result producing a higher correlation than others. The averaged signal that best correlates with the current signal allows the weight of the article to be read out from the data base.

5 Summary and Conclusion

We addressed the challenge of weighing articles on multiple support keys in a variety of ways. In summary the three questions posited in Section 1 are answered as follows.

1. Currently, there are two measuring concepts—parallel and serial—with which articles are measured. Which of the two measuring set-ups—single

or dual load cell—provides a higher accuracy?

We found that the doubling of time on the load cell that is consequent upon using staggered keys does improve weighing accuracy over the conventional single holder system used by COMPAC, when considering the low-pass filtered signal provided by the load cells (Section 1.2). The low-pass filter is too slow for the single holder at this conveyor belt speed, leading to a consistent under-estimation of the fruit weight for the single holder, as evidenced in Figure 6.

2. Can a mathematical model be developed that is able to estimate the true weight of the article from recorded data sets for all considered articles—single and multi-key alike?

   When the considered article is supported by more than one key, a static approach reveals that the weights recorded for each key should be added together. We found there was no detectable difference in accuracy, between adding the filtered signals before computing mass, and adding the computed masses from the separate filtered signals, as in Figure 6. However, if random noise is affecting the signal, then in principle we expect that adding raw signals before processing is better, as adding can lead to a partial noise cancellation effect.

   We see some evidence (Figure 4a) that articles supported by more than one key are sometimes rocking or bouncing off one key, which reduces the accuracy with which the mass might be estimated from the load-cell signal. It may be useful to try to model the nonlinear dynamics of bouncing and rocking, to identify when it may be occurring and possibly to indicate how to modify the signal processing required to obtain improved mass estimates during bouncing or rocking.

   We consider the mathematical models developed in this paper suitable for measuring single and multi-key articles. However, we suggest that a technological solution be found to prevent bouncing of articles on the keys.

3. What is the estimated theoretical weighing accuracy for a given conveyor belt velocity?

   With a view to using a filter that acts faster than the low-pass filter currently used, we considered two different approaches. A simple geometric approach gives very fast filtering that looks promising for removing much of the effect of oscillations at the natural frequency of the load and key and load-cell.

   We also considered a more sophisticated approach, fitting multi-parameter damped harmonic motion plus a step function to successive segments of the raw signal coming from one load-cell, using the Levenberg–Marquardt method with carefully chosen initial conditions to assist convergence. The results are very promising, providing very rapid filtering of the signal as illustrated by the piecewise step-functions in Figure 16. The filtered signal (the step-functions) that is visible in this figure, when viewed over the entire time-period that a key is on the load-cell, appears to be decaying steadily. This decay might indicate that the window used to fit the decaying signal is too narrow, and that a wider window might give better estimates of the decay rate, resulting in filtered signals that are closer to constant and that provide a more accurate measure of weight.

Acknowledgements We are grateful for the support and sponsorship of Victoria University of Wellington, KiwiNet including Seumas McCroskery, ANZIAM New Zealand Branch, the Centre for Maths in Industry, the New Zealand Mathematical Society, the MINZ Directors including Professor Graeme Wake, Compac Limited for the data used, especially Andrew McIntyre and Ben Goodger from Compac, and the other team members of our international study group, including David Waters, June-Yub Lee, Masahiro Yamamoto, Xudong Liu, and Rose Davies.

References

[1] MINZ-2004, Case Study Compac. http://www.minz.org.nz/assets/downloads/Case-Study-Compac.pdf M330

[2] Kesilmis, Z., & Baran, T. (2016). *A Geometric Approach to Beam Type Load Cell Response for Fast Weighing.* doi:10.1007/s12647-016-0168-2 M340, M342

[3] K. Levenberg, A method for the solution of certain non-linear problems in least squares. *Quarterly of applied mathematics*, 2(1944), pp. 164–168. http://www.jstor.org/stable/43633451 M349

[4] D. W. Marquardt, An algorithm for least-squares estimation of nonlinear parameters. *Journal of the society for Industrial and Applied Mathematics*, 11(1963), pp. 431–441. doi:10.1137/0111030 M349

Author addresses

1. **Stefanie Gutschmidt**, University of Canterbury, Christchurch, NEW ZEALAND.
mailto:stefanie.gutschmidt@canterbury.ac.nz
orcid:0000-0002-1528-809X

2. **Mark McGuinness**, Victoria University of Wellington, NEW ZEALAND.
mailto:mark.mcguinness@vuw.ac.nz
orcid:0000-0003-1860-6177

3. **William Munn**, Victoria University of Wellington, NEW ZEALAND.
mailto:munnwill@gmail.com

4. **James Hannam**, The University of Auckland, Auckland, NEW ZEALAND.

mailto:dr.e.enigma@gmail.com
orcid:0000-0003-3756-120X

5. **Emma Greenbank**, Victoria University of Wellington, New Zealand.
mailto:emma.greenbank@gmail.com
orcid:0000-0002-2332-3844

6. **Soomin Jeon**, KAIST, Daejeon, 34141, Korea.
mailto:soominjeon@kaist.ac.kr
orcid:0000-0003-1009-8227

7. **Chang-Ock Lee**, KAIST, Daejeon, 34141, Korea.
mailto:colee@kaist.edu
orcid:0000-0002-4704-9499

8. **Celia Kueh**, Massey University, Palmerston North, New Zealand.
mailto:celia.kueh@gmail.com
orcid:0000-0002-3505-803X

9. **Tony Gibb**, Adelaide Advanced Engineering, Adelaide, Australia.
mailto:agibb@351halifax.com

10. **Ben Goodger**, Compac Sorting Equipment Ltd., Auckland, New Zealand.

11. **Andrew McIntyre**, Compac Sorting Equipment Ltd., Auckland, New Zealand.